C Journal of Carbon Research

MDPI

Article

Application of L-FDM Technology to the Printing of Tablets That Release Active Substances—Preliminary Research

Ewa Gabriel [1,2], Anna Olejnik [1,2], Bogna Sztorch [2], Miłosz Frydrych [2], Olga Czerwińska [3], Robert Pietrzak [1] and Robert E. Przekop [2,*]

[1] Faculty of Chemistry, Adam Mickiewicz University in Poznan, 8 Uniwersytetu Poznanskiego, 61-614 Poznan, Poland; ewa.gabriel@amu.edu.pl (E.G.); anna.olejnik@amu.edu.pl (A.O.)
[2] Centre for Advanced Technologies, Adam Mickiewicz University in Poznan, 10 Uniwersytetu Poznanskiego, 61-614 Poznan, Poland; bogna.sztorch@amu.edu.pl (B.S.); frydrych@amu.edu.pl (M.F.)
[3] Sygnis S.A., Al. Grunwaldzka 472, 80-309 Gdansk, Poland; olga.czerwinska@sygnis.pl
* Correspondence: robert.przekop@amu.edu.pl

Abstract: The following work presents a method for obtaining PLA composites with activated carbon modified using the liquid for fused deposition modeling (L-FDM) method in which two different compounds, i.e., rhodamine and antipyrine, are introduced. Tablets saturated with substances were obtained. Microscopic tests were carried out, and these confirmed the presence of substances that had been introduced into the polymer structure. UV-Vis spectra and observation of the active substance release process confirmed the relationship between the printing speed and the amounts of the compounds liberated from the tablets. Additionally, the contact angle of the PLA with activated carbon composites was characterized. The hydrophilic nature of the obtained composites favors an increase in the amounts of compounds released during the release process, which is a desirable effect. The surfaces and pores of the obtained materials were also analyzed. The incorporation of activated carbon into PLA results in a significant increase in its surface area. Investigations indicate that a novel approach for introducing chemicals into polymer matrices through the L-FDM method holds promise for the prospective fabrication of tablets capable of a controlled and customized release of substances tailored to individual requirements.

Keywords: L-FDM; liquid for fused deposition modeling; printed medicines; carbon composites

Citation: Gabriel, E.; Olejnik, A.; Sztorch, B.; Frydrych, M.; Czerwińska, O.; Pietrzak, R.; Przekop, R.E. Application of L-FDM Technology to the Printing of Tablets That Release Active Substances—Preliminary Research. *C* **2024**, *10*, 23. https://doi.org/10.3390/c10010023

Academic Editor: Giuseppe Cirillo

Received: 21 December 2023
Revised: 29 February 2024
Accepted: 4 March 2024
Published: 6 March 2024

1. Introduction

Additive manufacturing technologies, commonly known as 3D printing, provide possibilities for producing objects with highly complex and precise structures. Thanks to this property, many scientists see the potential of this technique in the field of medicine/pharmacy to produce personalized medications. In scientific articles, studies related to printed medications using methods such as SLS (selective laser sintering), stereolithography (SLA), DIW (direct ink writing), and FDM (fused deposition modeling) can be found [1–9]. The main advantages of using these techniques include the ability to create customized products that are tailored to the patient's specific condition, greater control over the structures of pills (making them easier to swallow), control over the shape and structure of the pills, and control over the level of release of active substances [10–18].

An article by F. Fina et al. [19] discusses the incorporation of SLS into a range of 3D printing technologies available for the commercial production of pharmaceuticals. Their research describes the possibility of using this technique to produce so-called orally disintegrating tablets (ODTs), which is an alternative method for those seeking a quick and easy administration route that enables patients to take tablets without the need for water. The characteristic features of ODTs include a low-density formulation, low crushing strength, and high porosity. However, the work of Leong et al. [20] explores the possibility of printing structures with specific porosity for prolonged drug release using blends of

polylactic acid and polycaprolactone. Moreover, it was found that laser power, scanning speed, and bed temperature play a crucial role in the printing process.

Another printing technique that may be used in the production of extended-release drugs is SLA. In a study by P.K. Sharma et al. [21], the primary research goal was to harness the advanced capabilities of vat polymerization (SLA) to develop berberine-loaded hydrogel nanoparticles (BBR-NPs) immobilized within a unit dose of nanocomposite monoliths. SLA was employed to nano-fabricate berberine BBR-NPs and incorporate these nanocarriers into a 3D-printed oral dosage form made of biocompatible and biodegradable materials. The process of loading BBR onto the NPs and immobilizing them in a 3D-printed pill resulted in sustained release behavior. This innovative approach has the potential to enhance the gastrointestinal absorption of BBR, minimize degradation, and improve its in vivo bioavailability. Their study describes a promising strategy for the SLA-assisted 3D printing of composites applicable in various drug delivery systems, including multimodal drug release and multi-compartment drug delivery systems.

The next two methods of drug printing presented below involve extruding material and depositing it layer-by-layer on the working table. Depending on the material used and its form, we can distinguish DIW, where the material is in the form of a dense paste, and FDM, which involves depositing melted material (thermoplastic polymers).

An article by Q. Li et al. [22] describes research on DIW 3D-printed tablets using a paste composed of hydroxypropylmethylcellulose (HPMC K4M) and hydroxypropylmethylcellulose (HPMC E15) as the hydrophilic matrices, along with microcrystalline cellulose (MCC PH101) as the extrusion molding agent. The objective of their research was to investigate the viability of utilizing 3D extrusion-based printing as a method for pharmaceutical manufacturing to create gastro-floating tablets. The designed tablet's unique low-density lattice structure extends its time in the stomach, improving its drug release rate and effectiveness. Their study demonstrated that commonly used pharmaceutical excipients could be effectively utilized in the 3D extrusion-based printing process at room temperature. The dissolution profiles unveiled the correlation between the infill percentage and the drug release pattern. The findings of this investigation indicated the capability of 3D extrusion-based printing to manufacture gastro-floating tablets, demonstrating a floating duration of over 8 h.

The 3D printing of objects using the fused deposition modeling (FDM) technique involves melting a thermoplastic polymer in the nozzle of the printing head, which is loaded in the form of a filament. To obtain a filament with the addition of active pharmaceutical ingredients (APIs), it is necessary to mix it in a plasticized form using the hot melt extrusion (HME) method. A study by M.Kozakiewicz-Latała et al. [23] presents a systematic approach to creating additively manufactured tablets with a high-melting point API (hydrochlorothiazide, HCT, Tm = 266–268 °C). The formulation incorporates two pharmaceutically approved polymers, polyvinyl alcohol (PVA) and hydroxypropyl methylcellulose acetate succinate (HPMCAS), each with unique technological and pharmaceutical properties. The formulation process integrates hot melt extrusion (HME) and melt extrusion (ME) techniques. Filaments containing a crystalline drug were observed to be brittle and easily fractured, contrasting with the elastic and easily processable nature of filaments incorporating the drug in an amorphous state through melt extrusion (ME). Notably, significant variations in mechanical properties were noted for the HPMCAS/TEC and PVA/SOR materials following API incorporation. The introduction of even a small amount of the crystalline component to the HPMCAS/TEC filaments resulted in a substantial decrease in their mechanical properties. Extensive preformulation efforts have led to the production of API-loaded filaments with optimal mechanical properties, facilitating the creation of 3D-printed tablets with a favorable dissolution profile. An in-depth analysis of hydrochlorothiazide (HCT) release from various drug dosage forms revealed that the enhanced release from 3D-printed tablets is influenced by the tablet's morphology, its disintegration mechanism, and the drug phase in the formulation. Considering the potential challenges of processing high-melting point APIs through combined hot melt extrusion

(HME) and ME, the proposed approach can be adapted for the successful processing of other high-melting point molecules.

An article by G.G. Buyukgoz et al. [24] describes research on adjusting the release of the drug griseofulvin (GF) from designed and 3D FDM-printed tablets. This involved a specially extruded filament with a content ranging from 0–30 wt%. GF in hydroxypropyl cellulose (HPC) was used as the building material. Their analysis indicated that the surface area to volume ratio (SA/V) is crucial, and that the use of HPC results in near zero-order release. The results suggest that design options other than changing the tablet size are needed to achieve the desired drug release from 3D-printed doses.

An alternative method to polymer blending in the hot melt extrusion (HME) process is described by A. Goyanes et al. [25]. These researchers employed a method involving immersing a commercially available PVA filament in a beaker with ethanol containing the drug, stirring it for 24 h, and drying it. Subsequently, the solubility of the drugs in ethanol was measured, and the concentration was analyzed using HPLC. Finally, tablets containing 5-aminosalicylic acid (5-ASA, mesalazine) and 4-aminosalicylic acid (4-ASA) were 3D-printed; the parameters of these tablets, such as their size, resolution, and infill percentage, were varied to obtain tablets with different characteristics. Moreover, the authors demonstrated that the release patterns they achieved can also be altered by choosing specific printing parameters. The infill percentage affects the dissolution profile, and reducing the infill percentage of the tablets can result in a quicker release of the drug.

The technique of avoiding exposing APIs to high temperatures is described in an article by R.C.R. Beck et al. [26]. Drug loading was accomplished through immersing the 3D-printed drug delivery systems in a liquid suspension of nanoparticles. The impact of the primary polymeric material of the tablets, the inclusion of a channeling agent, and the infill percentage on both drug loading and drug release profiles were assessed. This study introduced an innovative approach to transforming nanocapsule suspensions into solid dosage forms and demonstrated an effective 3D printing method to produce novel drug delivery systems, including personalized nanomedicines.

Personalized drug printing in the pharmaceutical industry faces certain regulatory challenges, particularly in terms of the need to adapt the system for collaborations with pharmacies and hospitals. Conversely, in the case of the mass production of drugs using 3D printing technology, there are still unclear issues related to the methods of conducting clinical trials and bioequivalence studies, and these are crucial for ensuring safety. Since these products are tailored to the individual characteristics of specific patients, the standard approach based on statistical analysis for a specified number of volunteers becomes difficult and costly, especially when conducting such studies for each individual patient. It is also important to adapt the printing process to the relevant hygienic and technological standards to avoid contamination and ensure the repeatability and reliability of the production process [27].

It is necessary to delve into the required regulatory pathways for all stages of drug manufacturing, from the approval of raw materials, devices, and software, to essential control tools and the environment. It is expected that drug products produced through 3D printing will, in general, adhere to similar regulatory standards for safety, effectiveness, quality, and submission requirements as any pharmaceutical product manufactured through alternative techniques [28].

On the other hand, an exciting innovation associated with 3D printing technology is the possibility of producing drugs on demand and on-site, thereby eliminating the need for long-term storage and stability testing. Furthermore, 3D printing easily adapts to continuous production, enabling the optimal utilization of production spaces. In this context, there is potential for the application of an innovative approach based on 3D printing technology for mass production [29].

Activated carbon (AC) is a material with an internal porous structure that results in a large surface area, high adsorption capacity, and special surface reactivity [30]. It is widely used in processes like filtration, separation, purification, and catalysis due to its unique properties and availability [31]. Moreover, thanks to its biocompatibility, it has been widely used for medicinal purposes, e.g., for the removal of toxins from drug poisoning, food poisoning, infected wounds, kidney diseases, and so on [32–34]. AC has also been used as a drug-releasing agent. The existing research shows that drug concentrations and side effects can be reduced by using AC to optimize release, making medicines more effective therapeutically [35]. Olivier et al. [36] conducted a study to determine the feasibility of using a fabric containing activated carbon (AC) and calcium-deficient hydroxyapatite as a dual drug release system for bone regeneration purposes. Their results showed that rats implanted with this fabric had significantly faster bone reconstruction. The material was found to effectively deliver the drug to the site of damage, thereby facilitating bone healing. Nazarkin et al. [37] conducted research on the release of drugs from electrospun nanofibers containing AC. Their work presented comprehensive studies of the materials obtained, which showed good biocompatibility and physicochemical properties. Their results suggest that these materials have potential applications in the field of long-term drug release.

Carbon materials such as the above-mentioned activated carbon, graphite, and carbon nanotubes are used as fillers in polymer composites [38]. Composites based on thermoplastic polymers find applications in 3D printing using the FDM technique. A study by S. Balou et al. [39] focused on the development of sustainable filaments for FDM 3D printing. The authors used activated carbon derived from plant waste, such as leaves, and mixed it with polyethylene terephthalate glycol (PETG). The resulting filaments were environmentally friendly and cost-effective, demonstrating significantly higher mechanical strength (over 30%) and thermal stability. Our previous work [40] described the manufacturing process of polylactide composites with the addition of graphite, which, due to increased wear resistance, can be used for the 3D printing of sliding spare parts. A paper by L. Yang et al. [41] describes research on FDM prints using a filament made of a PLA/carbon nanotube (CNT) composite. Their results indicated that the CNTs had a significant impact on the mechanical properties, such as increased flexural and tensile strength, as well as conductivity.

In this article, we propose a novel method for drug printing using a new technique based on FDM technology (Figure 1), first described in a 2023 article by R. Przekop et al. titled *Liquid for Fused Deposition Modeling Technique (L-FDM)—A Revolution in Application Chemicals to 3D Printing Technology: Color and Elements* [42]. The method does not require the use of traditional plastic processing equipment to introduce the API into the filament; instead, the printing and surface coating of the filament occur simultaneously [42,43]. Therefore, production is fast, does not require the use of large amounts of material and an active substance solution, and enables the printing of small batches of tablets. First, the filament is immersed in a solution of the active substance placed in a U-shaped glass tube. For this purpose, saturated solutions of rhodamine b and antipyrine in methanol were prepared. Mixing with the polymer material occurs in the 3D printer nozzle during tablet printing. The printed tablets, which had elaborate active surface structures, were subjected to release testing in a solvent. The release of rhodamine B was examined due to its intense color, which enabled a visual assessment of its ability to be absorbed and released from L-FDM prints. Antipyrine was used as the active pharmaceutical ingredient (API). In this study, a carbon composite was used to increase the specific surface area and the ability of the submerged filament to absorb liquids. Models with different surface structures were printed from a composite filament to investigate its impact on the hydrophilic–hydrophobic properties. This could be of significant importance in future studies on the release of API substances from L-FDM-printed drugs.

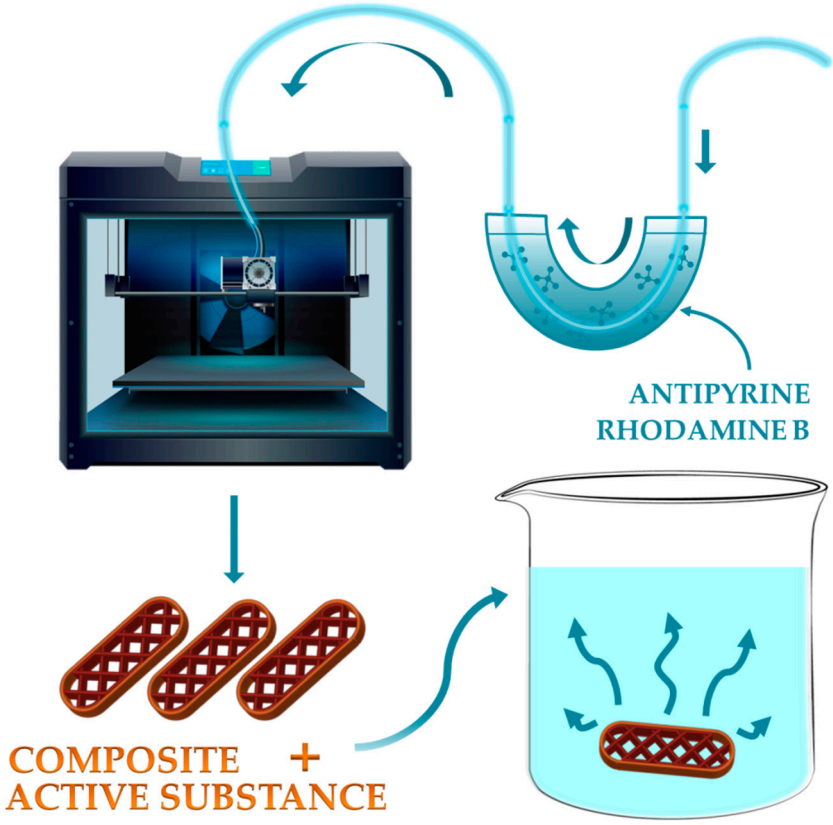

Figure 1. The concept of using L-FDM to print tablets that release active substances.

This study is the first attempt to explore the potential use of the new L-FDM technique as a tool for incorporating APIs into polymers, and to evaluate their how well they are released from the prints.

2. Materials and Methods

2.1. Materials

Polylactide (PLA Ingeo™ Biopolymer 2003D, NatureWorks, Minnetonka, Minneapolis, MN, USA) was used as the matrix polymer. Activated carbon (CWZ 22) was obtained from P.P.H Stanlab (Lublin, Poland). The chemicals were purchased from the following sources: methanol (MeOH) was purchased from P.P.H Stanlab (Lublin, Poland), rhodamine B was purchased from Warchem (Warszawa, Poland), and antipyrine was purchased from Merck KGaA (Darmstadt, Germany).

2.2. Sample Preparation

2.2.1. Extrusion of Filament with 5% Activated Carbon Content

The process of mixing polylactide (PLA) with 5 wt% carbon fillers and extruding it into a filament was carried out using a twin-screw extrusion line with a HAAKE RheomexOS and a co-rotating twin-screw extruder with cylinder lengths of 40:1 = 640 mm. The extrusion process temperatures were 165 °C, 175 °C, 175 °C, 180 °C, 180 °C, 185 °C, 185 °C, 185 °C, 185 °C, 180 °C, and 180 °C (from the feed zone to the head).

2.2.2. Printing of Tiles with Different Top and Infill Patterns

Small tiles with dimensions of 20 × 20 × 2 mm and various surface and infill patterns were printed on a Creality Ender 5 (by Creality 3D) with a nozzle diameter 0.4 mm. A Prusa Slicer with a profile dedicated to the Ender 5 printer was used to generate files supported by the printer (Table 1).

Table 1. Printing parameters of printed tiles.

Parameter	Value	
Slicer	Prusa Slicer	
Layer height [mm]	0.2	
Printing temperature [°C]	210	
Bed temperature [°C]	60	
Number of shells	2	
Printing speed [mm/s]	40	
First layer speed [mm/s]	10	
Combine infill every [layer]	1	
	Tiles with different top infill pattern	Tiles with different infill pattern
Top/bottom solid layers	2/2	0/2
Infill type	monotonic	Cubic/gyroid/stars/Hilbert curve
Top infill type *	Monotonic/Archimedean chords/Hilbert curve/octagram spiral	-
Infill %	100	99

* The top infill pattern is generated by the slicer only for one outer layer.

2.2.3. L-FDM Printing Process

The L-FDM printing technology uses 3D FDM traditional printers commonly available on the Polish and global markets. This research used Creality Ender 5 (by Creality 3D) with a Bowden-type extruder. The printing parameters are shown in the Table 2.

Table 2. Printing parameters of L-FDM-printed tablets.

Parameter	Value
Slicer	Prusa Slicer
Layer height [mm]	0.2
Printing temperature [°C]	210
Bed temperature [°C]	60
Number of shells	2
Top/bottom solid layers	0
Retraction length [mm]/speed [mm/s]	6/60
Infill type	Rectlinear
Infill %	20
Combine infill every [layer]	1
Printing speed [mm/s]	10/20/40
First layer speed [mm/s]	10

Forty tablets were printed during a single process; below, in Figure 2, the arrangement of the tablets in the working area of the 3D printer is presented.

2.3. Analyses

Water contact angle (WCA) analysis was performed using the sessile drop technique (5 µL) at room temperature, and atmospheric pressure was measured with a Krüss DSA100 goniometer. Five independent measurements were performed for each sample, each with a 5 µL water drop, and the obtained results were averaged.

Light microscopy images of the printed tablets were taken using a KEYENCE VHX-7000 digital microscope (Keyence International, Mechelen, Belgium, NV/SA) with a VH-Z100R wide-angle zoom lens at ×100 magnification.

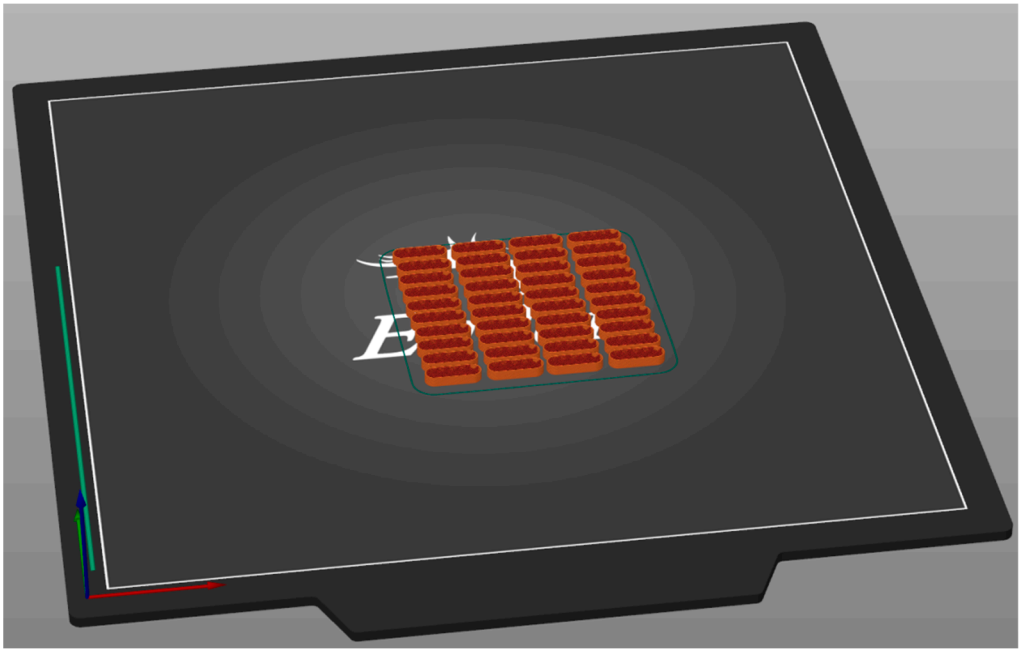

Figure 2. Screen from the slicer showing the arrangement of the tablets in the printer's working area.

Release studies were performed in methanol (100 mL) maintained at 30.0 ± 0.5 °C for 24 h. The absorbance of sample aliquots was measured to assess the amount of rhodamine and antipyrine released at each time point. The concentrations of the dissolved compounds were monitored using a UV-Vis spectrophotometer at 546 nm and 244 nm, respectively. Additionally, reference standard solutions of rhodamine and antipyrine in methanol were prepared to generate the calibration curves.

The textural characterizations of the powders, granules, and tablets were obtained via low-temperature nitrogen adsorption using a sorptometer Quantachrome® ASiQwin™ (Quantachrome Instruments, Boynton Beach, FL, USA). Before the adsorption–desorption isotherm measurements, the samples containing polymer were outgassed at 30 °C, and the activated carbon powder sample was outgassed at 150 °C for 48 h. The surface area was determined using the Brunauer–Emmett–Teller (BET) method, while the total pore volume and average pore diameter were calculated using the Barrett–Joyner–Halenda (BJH) method on the desorption branches of the isotherms.

3. Results and Discussion

3.1. WCAs of Tiles with Different Infill Patterns

To determine the impact of the fill structure on the hydrophilic–hydrophobic properties of the surface (Figures 3 and 4), a contact angle analysis was conducted. The results of the analysis of the contact angles of the prints from the composite filament containing 5% activated carbon in PLA are presented in Table 3. Samples with a top infill pattern exhibited lower contact angle values compared to tiles printed without top layers and with a 99% infill, indicating the higher affinity of the tested surface to water. Higher contact angle values were observed for measurements taken closer to the outer shell lines of the monotonic top infill tiles and in the middle of the top infill Archimedean chord patterns, i.e., in places where the surface of the tile is less flat and smooth. The higher contact angle values of the samples with different internal infill patterns may have resulted from increased roughness and surface irregularities on the tiles. Increased hydrophilicity is a desirable effect because it increases the release of the active substance from the printed objects.

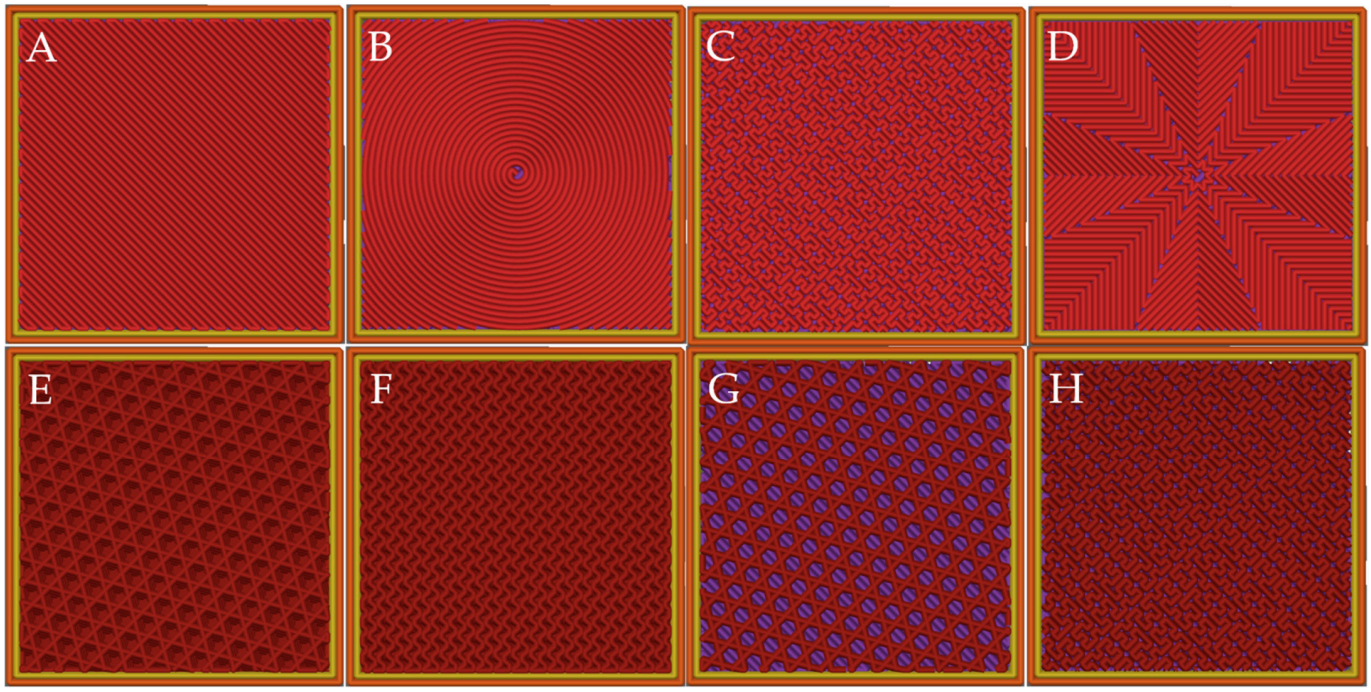

Figure 3. View of the tile surfaces after generating paths in the slicer. Type of top infill: (**A**) monotonic, (**B**) Archimedean chords, (**C**) Hilbert curve, (**D**) octagram spiral. Type of inner infill: (**E**) cubic, (**F**) gyroid, (**G**) stars, (**H**) Hilbert curve.

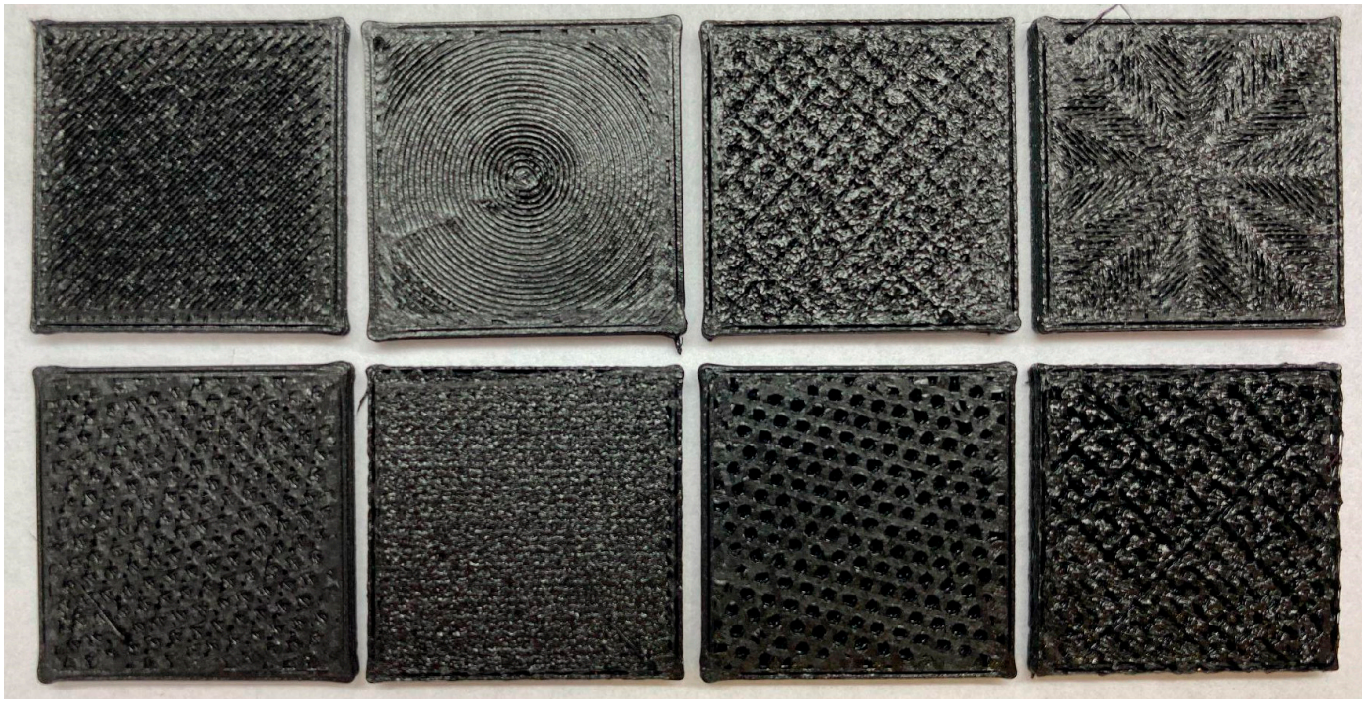

Figure 4. Photos of printed tiles with different fill patterns (tiles arranged in the same order as in Figure 3).

Table 3. Results of the water contact angle (WCA) analysis for printed composite tiles with different infill patterns.

Top Infill		Inner Infill	
Monotonic	92.66 ± 6.13	Cubic	96.18 ± 5.56
Archimedean chord	73.48 ± 6.56	Gyroid	73.88 ± 1.99
Hilbert curve	79.46 ± 6.94	Stars	81.02 ± 5.00
Octogram spiral	75.56 ± 6.88	Hilbert curve	81.48 ± 6.78

Immediate release occurs due to the dissolution of the active substance from the tablet surface. The presented results of the water contact angle analysis give preliminary indications of the impact of the surface on the future wetting capabilities. This can have a significant influence on the speed with which substances are released and the quantities in which they are released, depending on whether the tablet design contains API [44].

3.2. Microscopic Observation

The microscopic photos presented in Figure 5 compare the appearance of the printed reference tablet with activated carbon with the appearances of the tablets with added rhodamine. The most pronounced color change, correlating with the protracted printing duration, can be seen in (C) and (D). In the L-FDM technique, slower printing results in more contact with the modifier, causing greater adsorption.

A longer immersion time in the solution results in greater absorption into the immersed polymer, which, in the case of an API solution, also leads to increased absorption of the dissolved substance [45]. The rhodamine color gradually fades as the printing speed increases and the print quality deteriorates (E–H). The samples with antipyrine did not have any noticeable color differences, but only exhibited decreased print quality as the filament feed rate increased.

Figure 6 presents microscopic photos of the tablets after the release process. It can be seen that, apart from being deposited on the activated carbon, the rhodamine is also incorporated into the structure of the PLA matrix. The amount of released rhodamine directly depends on the printing speed (Figure 6A,B). At lower speeds, a higher dye content is observed in the composite, which is related to the more uniform structure of the printed object. As was described in the introduction, repeatability is a crucial aspect in drug production, and any defects observed in tablets can lead to differences in the speed with which active substances are released and the quantities in which they are released, as well as the quantity of delivered API within the tablet [27]. Moreover, it can be observed that there are fewer structural defects and air gaps by which rhodamine can be incorporated directly into the polymer structure. The rhodamine and antipyrine dissolution studies outlined in Section 3.3 confirm these observations of the substance release process. Antipyrine (Figure 6C,D) is adsorbed on activated carbon, and no significant changes are observed in the microscopic photos. However, substance release studies indicate that the process occurs in the opposite way in samples printed with rhodamine. It has been observed that at lower printing speeds, more active substance is released. This is related to the extension of the contact time of the active substance with the polymer, which makes the deposition process on activated carbon more effective.

3.3. Release Experiments

The rhodamine and antipyrine dissolution studies were performed using tablets printed at different speeds (10, 20, and 40 mm/s). The UV-Vis spectra were first recorded at certain time points to calculate the concentrations of both compounds released from PLA tablets, which incorporated 5% activated carbon. In Figures 7 and 8, the data registered after 15 min and 24 h of experiments are depicted. It was found that the absorbance increased for each tablet over time. However, it was also observed that the augmentation of the absorbance value was strictly related to the printing speed and the types of molecules introduced into the tablets. The absorbance data were then applied to calculate the con-

centrations of rhodamine and antipyrine released over time (Figure 9). For rhodamine, the slower the printed speed, the higher the amount of compound incorporated into the internal surface of the material. Rhodamine is a planar molecule that can be easily adsorbed due to the π–π interactions between the dyes' aromatic backbones and the skeletons of various materials [46]. In turn, antipyrine exhibited the opposite release behavior. The slower the printing speed, the higher the release of antipyrine from the tablets. This could be related to the weaker interactions between the composite and the drug molecules at the slowest printing speed compared to those of the tablets obtained at a faster printing speed.

Figure 5. Microscopic images presenting the surface morphologies of the PLA tablets made using the L-FDM method which incorporate a 5% concentration of activated carbon and which were modified with rhodamine. (**A**,**B**) reference sample, (**C**,**D**) tablet with rhodamine printed at 10 mm/s, (**E**,**F**) tablet with rhodamine printed at 20 mm/s, (**G**,**H**) tablet with rhodamine printed at 40 mm/s.

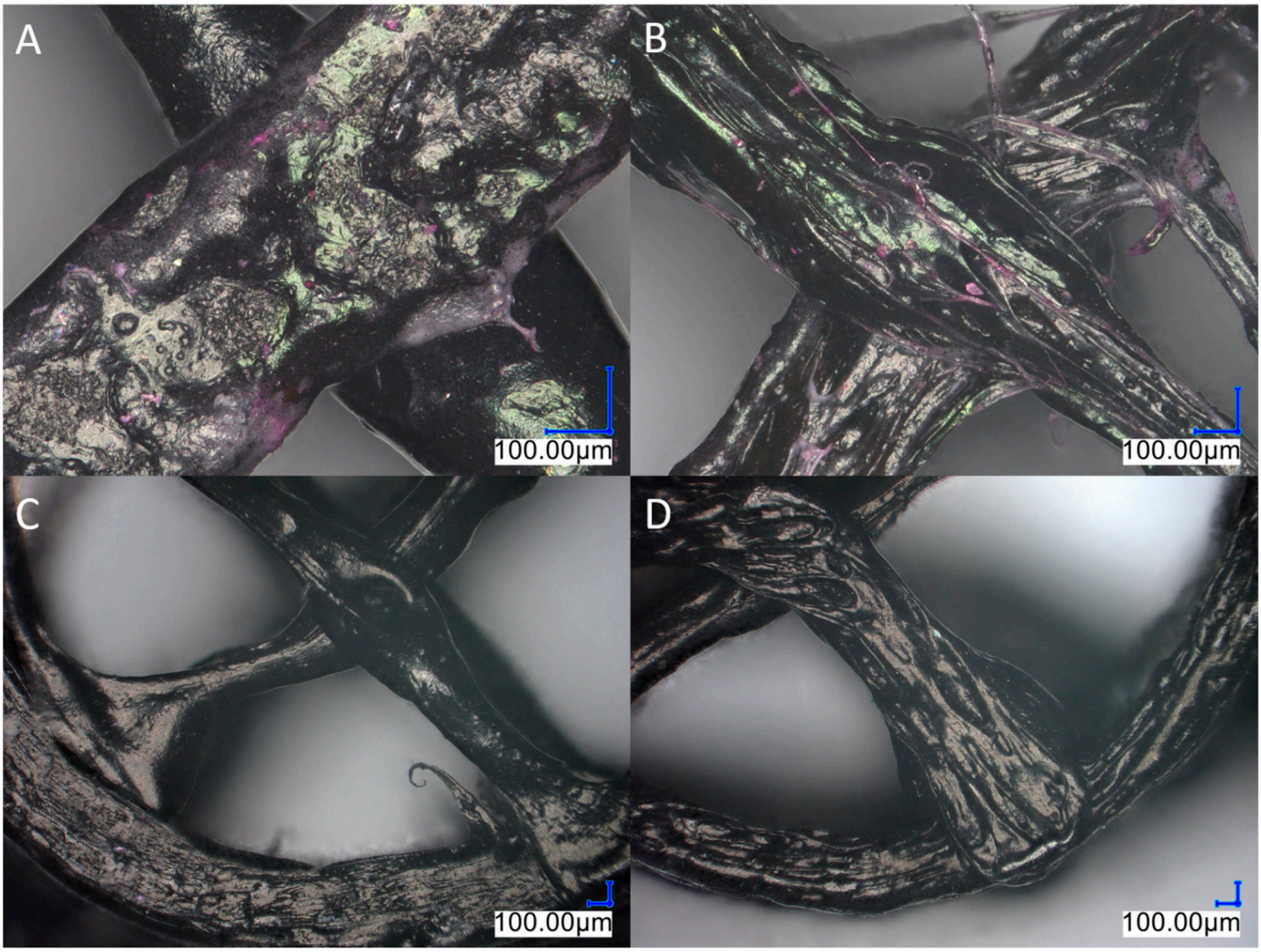

Figure 6. Microscopic images showing the surface morphologies of the PLA tablets after the release process. The tablets were made using the L-FDM method, incorporate a 5% concentration of activated carbon, and were modified with rhodamine (**A**,**B**) and antipyrine (**C**,**D**). (**A**) tablet with rhodamine printed at 10 mm/s, (**B**) tablet with rhodamine printed at 40 mm/s, (**C**) tablet with antipyrine printed at 10 mm/s, (**D**) tablet with antipyrine printed at 10 mm/s 40 mm/s.

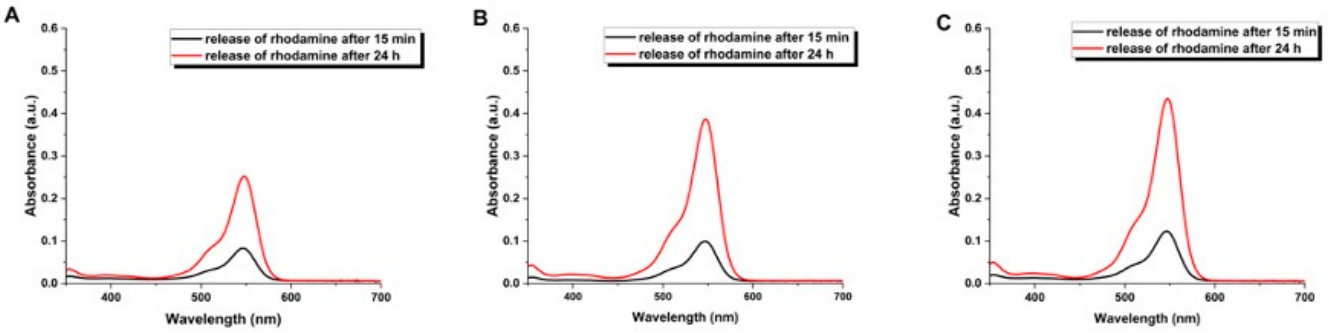

Figure 7. UV-Vis spectrum of rhodamine released from tablets printing speed 10 mm/s (**A**), 20 mm/s (**B**), 40 mm/s (**C**).

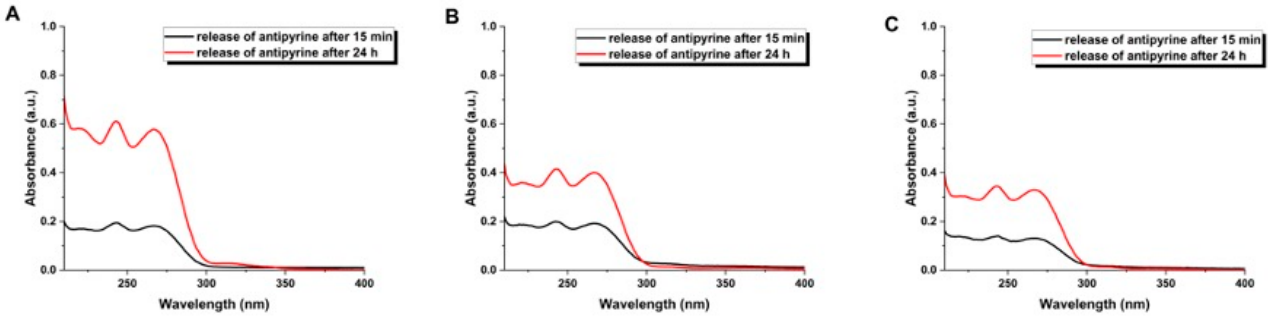

Figure 8. UV spectra of antipyrine released from tablets produced using printing speeds of 10 mm/s (**A**), 20 mm/s (**B**), and 40 mm/s (**C**).

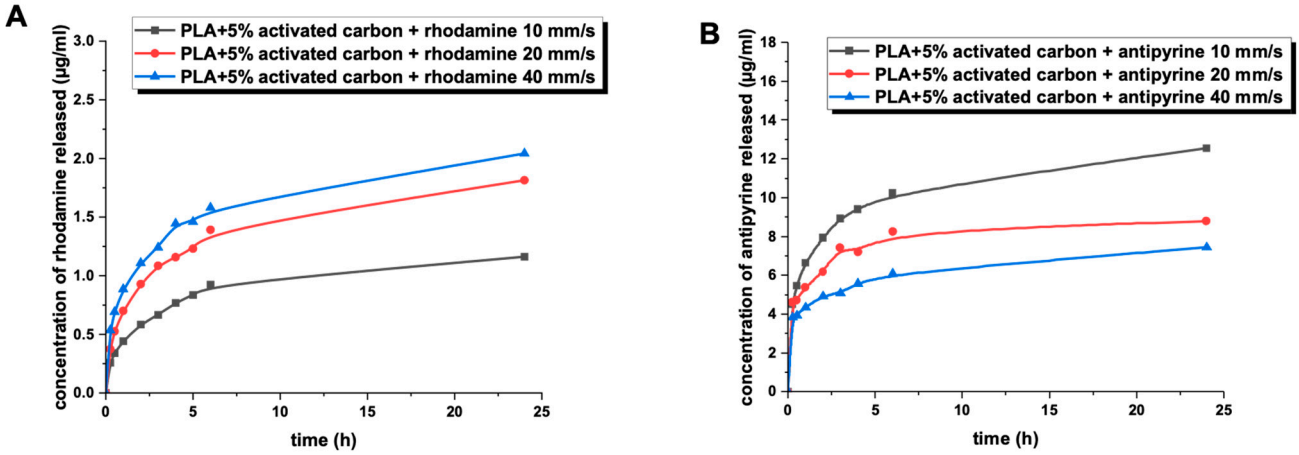

Figure 9. Concentrations of rhodamine (**A**) and antipyrine (**B**) released from tablets produced using printing speeds of 10 mm/s, 20 mm/s, and 40 mm/s.

3.4. Surface Area Characterization Using Low-Temperature Nitrogen Adsorption Analysis

In Figures 10 and 11, and in Table 4, the results of the surface area analysis, carried out using the Brunauer–Emmett–Teller (BET) method, as well as the total pore volume and average pore diameter, calculated using the Barrett–Joyner–Halenda (BJH) method, are presented. The changes in pore volume shown below are similar to those observed in the polymer without the addition of a filler, while the BET surface area increases for the composite. Carbon powder may form agglomerates, resulting in a more rugged composite surface. An increase in BET surface area can influence the amount a substance that is released, especially when it comes to active pharmaceutical ingredients (APIs). A larger surface with which the tablet can interact with the solvent can promote faster leaching of the active substance from the composite, which can accelerate the process of releasing the active substance. Therefore, understanding and controlling the BET surface area can be crucial in drug design, particularly when the rate of substance release is critical for therapeutic effectiveness.

Table 4. BET surface area, pore volume, and average pore diameter values of neat PLA granulate, activated carbon powder, and printed tablets.

Sample Name	BET Surface Area [m^2/g]	Pore Volume [cm^3/g]	Average Pore Diameter [nm]
PLA granulate	0	0.006	3.317
CA powder	779	0.202	3.938
CA 5% tablet	40	0.005	3.141

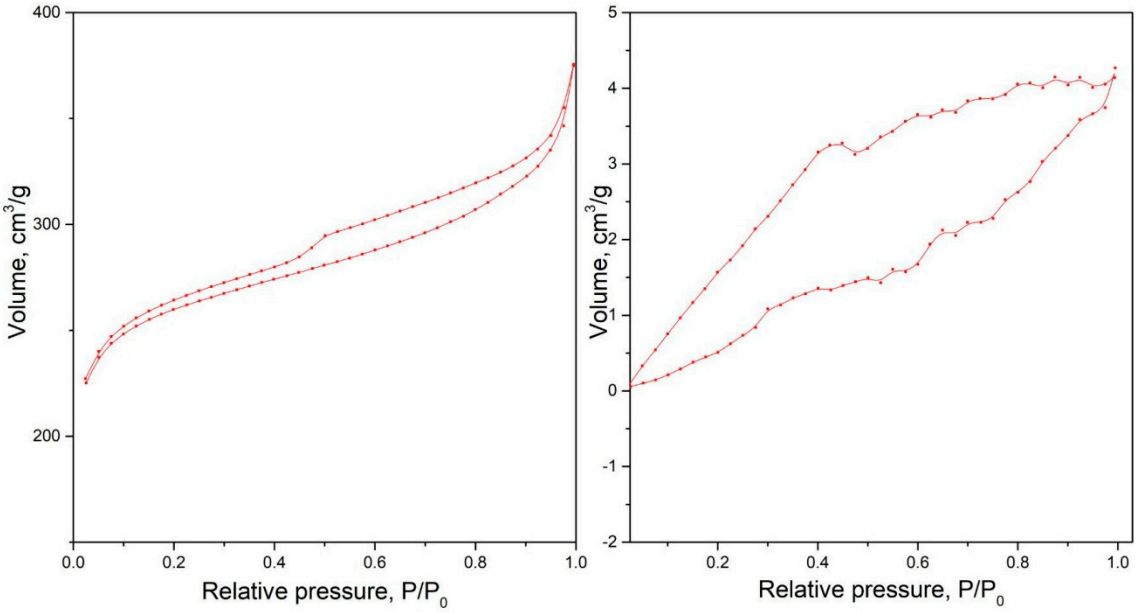

Figure 10. Low-temperature nitrogen adsorption–desorption isotherms for activated carbon (**left**) and printed tablets (**right**).

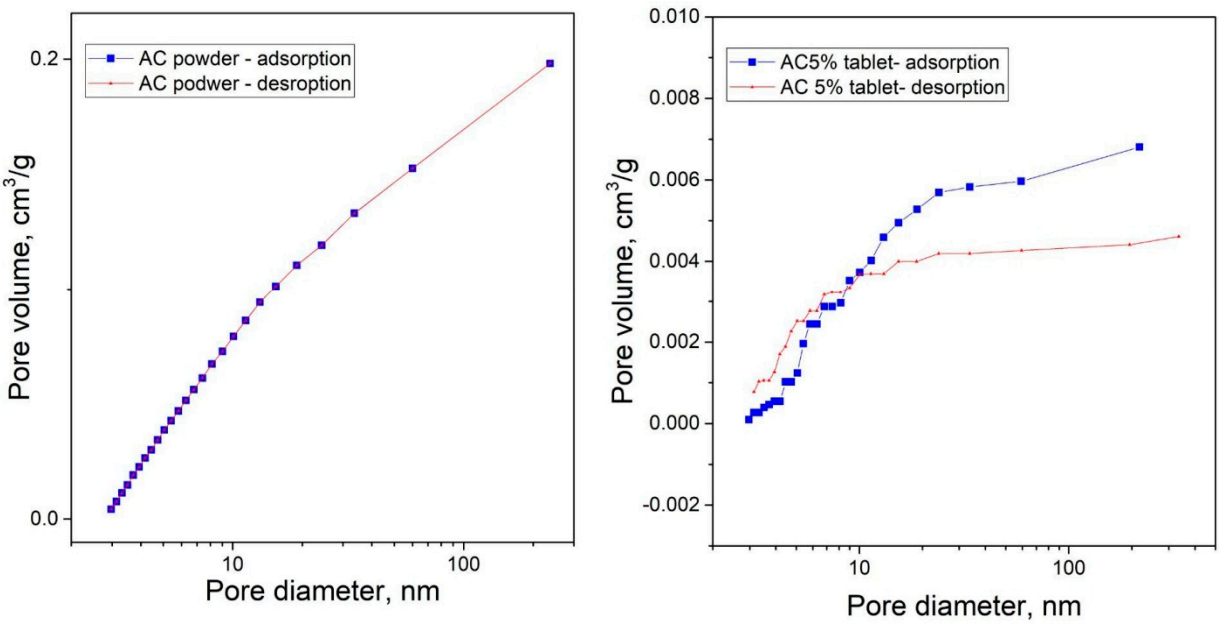

Figure 11. Pore volume distribution for activated carbon powder and printed tablets.

4. Conclusions

This article presents research in which, for the first time, the use of the L-FDM technique for printing personalized tablets containing active substances were investigated.

A filament with a 5% content of activated carbon in PLA was obtained. This was then used as a material with an increased capacity for solution adsorption after immersion. The results of the WCA studies confirmed the influence of the surface structure on the hydrophilic–hydrophobic properties of the printed parts. Microscopic observations confirmed the presence of rhodamine, which was introduced into the prints using the L-FDM technique. The study of the release of the active substance from the tablets printed using the L-FDM technique revealed a close dependence on the printing speed, the material from which the filament was made, and the type of molecules introduced into the tablets. Thanks

to these properties, further research on this topic may, in the future, lead to the development of drugs with a specific, personalized profile of active substance release. The addition of activated carbon to PLA results in an increase in the specific surface area. However, further research is needed to determine the impact of the physicochemical properties of the introduced carbons on the sorption capacity of the obtained filaments and the release of the active substances from the L-FDM-printed tablets. This research demonstrates that the use of a new technique for introducing chemical substances into polymer matrices using the L-FDM method may, in the future, be employed to produce tablets with the ability to release substances in a specific manner tailored to individual needs.

The studies described in the article may be significant in the field of pharmacy. However, the actual application potential of drugs printed using the L-FDM technique requires further extensive research. It is crucial to ensure the repeatability of the L-FDM printing of tablets in terms of the speed with which APIs are released and the quantities in which they are released. In this article, a PLA polymer was used as an example, but any thermoplastic filament can be used. The polymer and API must be compatible with each other; it is important for the API to exhibit temperature resistance during printing, and this is determined by the chosen thermoplastic polymer. The drug and polymer should be selected to avoid confounding effects arising from drug–polymer interactions. Further tests regarding drug printing using the L-FDM technique may focus on analyzing the impact of printing parameters, tablet structure, and the API–composite system employed on the speed with which APIs are released from the tablets and the quantities in which they are released. Additional studies are necessary, and these should emphasize a broader range of substance variations, pharmacokinetics, reproducibility, safety, and regulatory considerations. This is crucial for enabling the practical application of this technology.

Author Contributions: Conceptualization, R.E.P.; methodology, R.E.P.; software, E.G., M.F., A.O. and B.S.; validation, R.E.P. and B.S.; formal analysis, E.G., M.F., A.O. and B.S.; investigation, E.G., M.F., A.O. and O.C. resources, R.E.P.; data curation, R.E.P.; writing—original draft preparation, E.G., A.O., B.S., M.F. and R.P.; writing—review and editing, R.E.P.; visualization, E.G., A.O., M.F. and O.C.; supervision, R.E.P.; project administration, R.E.P. All authors have read and agreed to the published version of the manuscript.

Funding: This work was funded by the Smart Growth Operational Programme, project no. POIR.04.02.00-00-D003/20-00; European Funds, project no. RPWP.01.01.00-30-0004/18; and the Ministry of Science and Higher Education, project no. 21/529535/SPUB/SP/2022.

Data Availability Statement: Data are contained within the article.

Conflicts of Interest: Author Olga Czerwińska was employed by the company Sygnis S.A. The remaining authors declare that the research was conducted in the absence of any commercial or financial relationships that could be construed as a potential conflict of interest.

References

1. Kadry, H.; Al-Hilal, T.A.; Keshavarz, A.; Alam, F.; Xu, C.; Joy, A.; Ahsan, F. Multi-Purposable Filaments of HPMC for 3D Printing of Medications with Tailored Drug Release and Timed-Absorption. *Int. J. Pharm.* **2018**, *544*, 285–296. [CrossRef]
2. Quodbach, J.; Bogdahn, M.; Breitkreutz, J.; Chamberlain, R.; Eggenreich, K.; Elia, A.G.; Gottschalk, N.; Gunkel-Grabole, G.; Hoffmann, L.; Kapote, D.N.; et al. Quality of FDM 3D Printed Medicines for Pediatrics: Considerations for Formulation Development, Filament Extrusion, Printing Process and Printer Design. *Ther. Innov. Regul. Sci.* **2021**, *56*, 910–928. [CrossRef]
3. Amekyeh, H.; Tarlochan, F.; Billa, N. Practicality of 3D Printed Personalized Medicines in Therapeutics. *Front. Pharmacol.* **2021**, *12*, 646836. [CrossRef]
4. Chen, G.; Xu, Y.; Kwok, P.C.L.; Kang, L. Pharmaceutical Applications of 3D Printing. *Addit. Manuf.* **2020**, *34*, 101209. [CrossRef]
5. Haris, M.S.; Azlan, N.H.M.; Taher, M.; Rus, S.M.; Chatterjee, B. 3D-Printed Drugs: A Fabrication of Pharmaceuticals towards Personalized Medicine. *Indian J. Pharm. Educ. Res.* **2020**, *54*, s411–s422. [CrossRef]
6. Abaci, A.; Gedeon, C.; Kuna, A.; Guvendiren, M. Additive Manufacturing of Oral Tablets: Technologies, Materials and Printed Tablets. *Pharmaceutics* **2021**, *13*, 156. [CrossRef]
7. Agrawal, A.; Gupta, A.K. 3D printing technology in pharmaceuticals and biomedical: A review. *J. Drug Deliv. Ther.* **2019**, *9*, 1–4.
8. Kantaros, A. 3D Printing in Regenerative Medicine: Technologies and Resources Utilized. *Int. J. Mol. Sci.* **2022**, *23*, 14621. [CrossRef]

9. Melčová, V.; Svoradová, K.; Menčík, P.; Kontárová, S.; Rampichová, M.; Hedvičáková, V.; Sovková, V.; Přikryl, R.; Vojtová, L. FDM 3D Printed Composites for Bone Tissue Engineering Based on Plasticized Poly(3-hydroxybutyrate)/poly(D,L-lactide) Blends. *Polymers* **2020**, *12*, 2806. [CrossRef] [PubMed]
10. Afsana; Jain, V.; Haider, N.; Jain, K. 3D Printing in Personalized Drug Delivery. *Curr. Pharm. Des.* **2019**, *24*, 5062–5071. [CrossRef] [PubMed]
11. Kantaros, A.; Ganetsos, T.; Petrescu, F.I.T. Transforming Object Design and Creation: Biomaterials and Contemporary Manufacturing Leading the Way. *Biomimetics* **2024**, *9*, 48. [CrossRef] [PubMed]
12. Mathew, E.; Pitzanti, G.; Larrañeta, E.; Lamprou, D.A. 3D Printing of Pharmaceuticals and Drug Delivery Devices. *Pharmaceutics* **2020**, *12*, 266. [CrossRef] [PubMed]
13. Deshmane, S.V.; Kendre, P.N.; Mahajan, H.S.; Jain, S.P. Stereolithography 3D Printing Technology in Pharmaceuticals: A Review. *Drug Dev. Ind. Pharm.* **2021**, *47*, 1362–1372. [CrossRef] [PubMed]
14. Shi, K.; Salvage, J.P.; Maniruzzaman, M.; Nokhodchi, A. Role of Release Modifiers to Modulate Drug Release from Fused Deposition Modelling (FDM) 3D Printed Tablets. *Int. J. Pharm.* **2021**, *597*, 120315. [CrossRef] [PubMed]
15. Zhu, X.; Li, H.; Huang, L.; Zhang, M.; Fan, W.; Cui, L. 3D printing promotes the development of drugs. *Biomed. Pharmacother.* **2020**, *131*, 110644. [CrossRef] [PubMed]
16. Yu, D.G.; Branford-White, C.; Yang, Y.C.; Zhu, L.M.; Welbeck, E.W.; Yang, X.L. A novel fast disintegrating tablet fabricated by three-dimensional printing. *Drug Dev. Ind. Pharm.* **2009**, *35*, 1530–1536. [CrossRef] [PubMed]
17. Goyanes, A.; Buanz, A.B.; Basit, A.W.; Gaisford, S. Fused-filament 3D printing (3DP) for fabrication of tablets. *Int. J. Pharm.* **2014**, *476*, 88–92. [CrossRef]
18. Tan, Y.J.N.; Yong, W.P.; Kochhar, J.S.; Khanolkar, J.; Yao, X.; Sun, Y.; Ao, C.K.; Soh, S. On-demand fully customizable drug tablets via 3D printing technology for personalized medicine. *J. Control. Release* **2020**, *322*, 42–52. [CrossRef]
19. Fina, F.; Goyanes, A.; Gaisford, S.; Basit, A.W. Selective laser sintering (SLS) 3D printing of medicines. *Int. J. Pharm.* **2017**, *529*, 285–293. [CrossRef]
20. Leong, K.F.; Chua, C.K.; Gui, W.S.; Verani. Building porous biopolymeric microstructures for controlled drug delivery devices using selective laser sintering. *Int. J. Adv. Manuf. Technol.* **2006**, *31*, 483–489. [CrossRef]
21. Sharma, P.K.; Choudhury, D.; Yadav, V.; Murty, U.S.N.; Banerjee, S. 3D printing of nanocomposite pills through desktop vat photopolymerization (stereolithography) for drug delivery reasons. *3D Print. Med.* **2022**, *8*, 3. [CrossRef]
22. Li, Q.; Guan, X.; Cui, M.; Zhu, Z.; Chen, K.; Wen, H.; Jia, D.; Hou, J.; Xu, W.; Yang, X.; et al. Preparation and investigation of novel gastro-floating tablets with 3D extrusion-based printing. *Int. J. Pharm.* **2018**, *535*, 325–332. [CrossRef] [PubMed]
23. Kozakiewicz-Latała, M.; Junak, A.; Złocińska, A.; Pudło, W.; Prusik, K.; Szymczyk-Ziółkowska, P.; Karolewicz, B.; Nartowski, K.P. Adjusting the melting point of an Active Pharmaceutical Ingredient (API) via cocrystal formation enables processing of high melting drugs via combined hot melt and materials extrusion (HME and ME). *Addit. Manuf.* **2022**, *60*, 103196. [CrossRef]
24. Buyukgoz, G.G.; Soffer, D.; Defendre, J.; Pizzano, G.M.; Davé, R.N. Exploring tablet design options for tailoring drug release and dose via fused deposition modeling (FDM) 3D printing. *Int. J. Pharm.* **2020**, *591*, 119987. [CrossRef] [PubMed]
25. Goyanes, A.; Buanz, A.B.; Hatton, G.B.; Gaisford, S.; Basit, A.W. 3D printing of modified-release aminosalicylate (4-ASA and 5-ASA) tablets. *Eur. J. Pharm. Biopharm.* **2015**, *89*, 157–162. [CrossRef] [PubMed]
26. Beck, R.C.R.; Chaves, P.S.; Goyanes, A.; Vukosavljevic, B.; Buanz, A.; Windbergs, M.; Basit, A.W.; Gaisford, S. 3D printed tablets loaded with polymeric nanocapsules: An innovative approach to produce customized drug delivery systems. *Int. J. Pharm.* **2017**, *528*, 268–279. [CrossRef] [PubMed]
27. Melocchi, A.; Briatico-Vangosa, F.; Uboldi, M.; Parietti, F.; Turchi, M.; von Zeppelin, D.; Maroni, A.; Zema, L.; Gazzaniga, A.; Zidan, A. Quality considerations on the pharmaceutical applications of fused deposition modeling 3D printing. *Int. J. Pharm.* **2021**, *592*, 119901. [CrossRef]
28. Awad, A.; Trenfield, S.J.; Gaisford, S.; Basit, A.W. 3D printed medicines: A new branch of digital healthcare. *Int. J. Pharm.* **2018**, *548*, 586–596. [CrossRef]
29. Kantaros, A.; Ganetsos, T. From Static to Dynamic: Smart Materials Pioneering Additive Manufacturing in Regenerative Medicine. *Int. J. Mol. Sci.* **2023**, *24*, 15748. [CrossRef]
30. Park, S.; Kim, B. A study on NO removal of activated carbon fibers with deposited silver nanoparticles. *J. Colloid Interface Sci.* **2005**, *282*, 124–127. [CrossRef]
31. Hung, M.; Yuan, S.; Chang, S.I.; Liao, J.; Ko, T.; Cheng, C. Evaluation of active carbon fibers used in cell biocompatibility and rat cystitis treatment. *Carbon* **2014**, *68*, 628–637. [CrossRef]
32. Verma, C.; Quraishi, M.A. *Activated Carbon*; The Royal Society of Chemistry: London, UK, 2023. [CrossRef]
33. Ovington, L.G. Advances in wound dressings. *Clin. Dermatol.* **2006**, *25*, 33–38. [CrossRef]
34. Lewoyehu, M. Comprehensive review on synthesis and application of activated carbon from agricultural residues for the remediation of venomous pollutants in wastewater. *J. Anal. Appl. Pyrolysis* **2021**, *159*, 105279. [CrossRef]
35. Yadavalli, T.; Ames, J.; Agelidis, A.; Suryawanshi, R.; Jaishankar, D.; Hopkins, J.; Thakkar, N.; Koujah, L.; Shukla, D. Drug-encapsulated carbon (DECON): A novel platform for enhanced drug delivery. *Sci Adv.* **2019**, *5*, eaax0780. [CrossRef] [PubMed]
36. Olivier, F.; Bonnamy, S.; Rochet, N.; Drouet, C. Activated Carbon Fiber Cloth/Biomimetic Apatite: A Dual Drug Delivery System. *Int. J. Mol. Sci.* **2021**, *22*, 12247. [CrossRef]

37. Nazarkina, Z.K.; Stepanova, A.O.; Chelobanov, B.P.; Kvon, R.I.; Simonov, P.A.; Karpenko, A.A.; Laktionov, P.P. Activated Carbon-Enriched Electrospun-Produced Scaffolds for Drug Delivery/Release in Biological Systems. *Int. J. Mol. Sci.* **2022**, *24*, 6713. [CrossRef] [PubMed]
38. Sztorch, B.; Brząkalski, D.; Pakuła, D.; Frydrych, M.; Špitalský, Z.; Przekop, R.E. Natural and Synthetic Polymer Fillers for Applications in 3D Printing—FDM Technology Area. *Solids* **2022**, *3*, 508–548. [CrossRef]
39. Balou, S.; Ahmed, I.; Priye, A. From Waste to Filament: Development of Biomass-Derived Activated Carbon-Reinforced PETG Composites for Sustainable 3D Printing. *ACS Sustain. Chem. Eng.* **2023**, *11*, 12667–12676. [CrossRef]
40. Przekop, R.E.; Kujawa, M.; Pawlak, W.; Dobrosielska, M.; Sztorch, B.; Wieleba, W. Graphite Modified Polylactide (PLA) for 3D Printed (FDM/FFF) Sliding Elements. *Polymers* **2020**, *12*, 1250. [CrossRef]
41. Yang, L.; Li, S.; Zhou, X.; Liu, J.; Li, Y.; Yang, M.; Yuan, Q.; Zhang, W. Effects of carbon nanotube on the thermal, mechanical, and electrical properties of PLA/CNT printed parts in the FDM process. *Synth. Met.* **2019**, *253*, 122–130. [CrossRef]
42. Przekop, R.E.; Gabriel, E.; Pakuła, D.; Sztorch, B. Liquid for Fused Deposition Modeling Technique (L-FDM)—A Revolution in Application Chemicals to 3D Printing Technology: Color and Elements. *Appl. Sci.* **2023**, *13*, 7393. [CrossRef]
43. Przekop, R.E.; Gabriel, E.; Pakuła, D.; Sztorch, B. Liquid to Fused Deposition Modeling (L-FDM)—A Revolution in Application Chemicals to 3D Printing Technology—Mechanical and Functional Properties. *Appl. Sci.* **2023**, *13*, 8462. [CrossRef]
44. Bettini, R.; Catellani, P.L.; Santi, P.; Massimo, G.; Peppas, N.A.; Colombo, P. Translocation of drug particles in HPMC matrix gel layer: Effect of drug solubility and influence on release rate. *J. Control. Release* **2001**, *70*, 383–391. [CrossRef]
45. Kamaludin, N.H.I.; Ismail, H.; Rusli, A.; Ting, S.S. Thermal behavior and water absorption kinetics of polylactic acid/chitosan biocomposites. *Iran Polym. J.* **2021**, *30*, 135–147. [CrossRef]
46. Zghal, S.; Jedidi, I.; Cretin, M.; Cerneaux, S.; Abdelmouleh, M. Adsorptive Removal of Rhodamine B Dye Using Carbon Graphite/CNT Composites as Adsorbents: Kinetics, Isotherms and Thermodynamic Study. *Materials* **2023**, *16*, 1015. [CrossRef]